Proceedings of ASME Turbo Expo 2010: Power for Land, Sea and Air
GT2010
June 14-18, 2010, Glasgow, UK

GT2010-23023

EXPERIMENTAL INVESTIGATION OF THE NONLINEAR RESPONSE OF SWIRL STABILIZED FLAMES TO EQUIVALENCE RATIO OSCILLATIONS

Kyu Tae Kim*, Jong Guen Lee, Bryan D. Quay, and Domenic A. Santavicca
Center for Advanced Power Generation
Department of Mechanical and Nuclear Engineering
The Pennsylvania State University, University Park, PA, 16802

ABSTRACT

The nonlinear response of a swirl-stabilized flame to equivalence ratio oscillations was experimentally investigated in an atmospheric-pressure, high-temperature, lean-premixed model gas turbine combustor. To generate high-amplitude equivalence ratio oscillations, fuel was modulated using a siren type modulating device. The mixture ratio oscillations at the inlet of the combustion chamber were measured by the infrared absorption technique and the flame's response, i.e., the fluctuation in the flame's rate of heat release, was estimated by CH* chemiluminescence emission intensity. Phase-resolved CH* chemiluminescence images were taken to characterize the dynamic response of the flame. Results show that the amplitude and frequency dependence of the flame's response to equivalence ratio oscillations is qualitatively consistent with the flame's response to inlet velocity oscillations. The underlying physics of the nonlinear response of the flame to equivalence ratio oscillations, however, is associated with the intrinsically nonlinear dependence of the heat of reaction and burning velocity on the equivalence ratio. It was found that combustion cannot be sustained under conditions of high amplitude equivalence ratio oscillations. Lean blowoff occurs when the normalized amplitude of the equivalence ratio oscillation exceeds a threshold value. The threshold value is dependent on the mean equivalence ratio and modulation frequency.

INTRODUCTION

Lean premixed combustion has been successful in meeting current NOx emissions regulations; however, this has been achieved at the expense of increased combustion dynamics. Combustion instabilities are characterized by large amplitude pressure oscillations that are driven by unsteady heat release. Because of limitations in our understanding of the fundamentals of combustion dynamics, it is currently not possible to design a lean premixed gas turbine combustor that is stable over its entire operating range, or to even predict the instability characteristics (frequency and intensity) of a given system at the development state. As a result, in-field modifications to the engines are typically required so as to navigate around unstable operating conditions or to protect the system from high amplitude pressure oscillations. Such solutions can be time-consuming, expensive and often compromise the system's performance. Therefore, the successful development of the next generation of ultra-low emissions lean-premixed gas turbine engines requires a complete understanding of the nature of combustion instabilities, and design tools that are based on accurate physics-based flame response models.

Over the last two decades, extensive research has been performed to investigate the mechanisms that drive combustion instability [1]. The most significant contributing factors include flame surface area fluctuations driven by acoustic velocity oscillations [2-4], large scale vortex structures [5-8], flame-wall interaction [9], and equivalence ratio oscillations [10-13]. Recently, related studies have been performed to examine the effect of inlet velocity perturbations induced by acoustic waves on the response of a premixed flame [14-17]. Flame transfer functions which describe the amplitude-dependent response characteristics of a flame and the influence of large scale coherent structures on the flame's nonlinear response were experimentally determined. Numerical simulations have been also performed to compare with measured flame transfer functions [18]. The response of a flame to acoustic excitation and the interaction of the flame w-

* Corresponding author: University of Cambridge, Engineering Department, Trumpington Street, Cambridge, CB2 1PZ, UK. E-mail address: ktk23@cam.ac.uk.

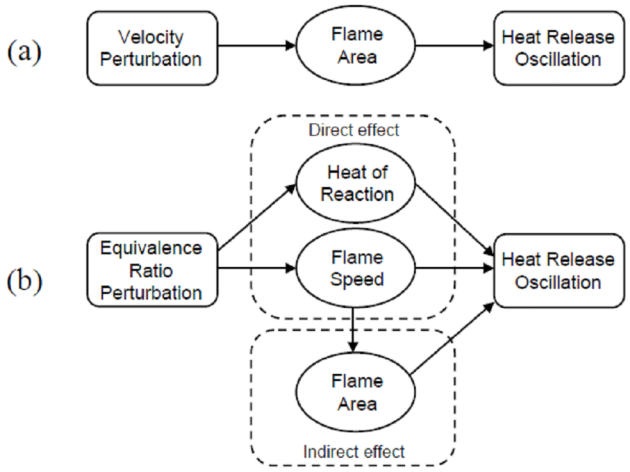

Figure 1. Mechanism of the flame response to (a) velocity perturbations and (b) equivalence ratio perturbations [12].

ith coherent structures induced by strong acoustic forcing are now well understood.

To date, however, the response of a swirl-stabilized lean-premixed flame to equivalence ratio modulations has not been well explored experimentally. Making simultaneous measurements of the temporal fluctuations of equivalence ratio and the flame's heat release response is a challenging problem. Generating large amplitude oscillations of equivalence ratio in the mixing section, while keeping the amplitude of velocity fluctuations negligible, is also a difficult task. Due to these limitations in experimental investigations, the response of a flame to equivalence ratio modulation has been treated analytically or numerically. Cho and Lieuwen [12] performed a complete analysis of the major sources of heat release for a laminar premixed flame subjected to equivalence ratio oscillations. They concluded that the heat release response is controlled by the superposition of three disturbances: heat of reaction, flame speed, and flame area. As illustrated schematically in Figure 1, fluctuations of the heat of reaction and burning velocity are directly generated by equivalence ratio oscillations. Flame area has an indirect influence on heat release, because it is generated by flame speed fluctuations. Recently, Birbaud et al. [19] numerically investigated the nonlinear dynamics of an inverted laminar dihedral flame spreading in an open geometry when the flame is submitted to equivalence ratio modulations. They reported that the rapid burning of fresh mixture pockets generates a nonlinear heat release signal with abrupt changes in the waveform. Sengissen et al. [20] studied the response of swirled partially premixed flames to fuel flow rate modulations using large eddy simulation (LES). They described no noticeable saturation effect: the flame behaves linearly up to amplitude of 80%.

In the present paper, the response of a turbulent swirl stabilized flame to equivalence ratio oscillations is experiment-

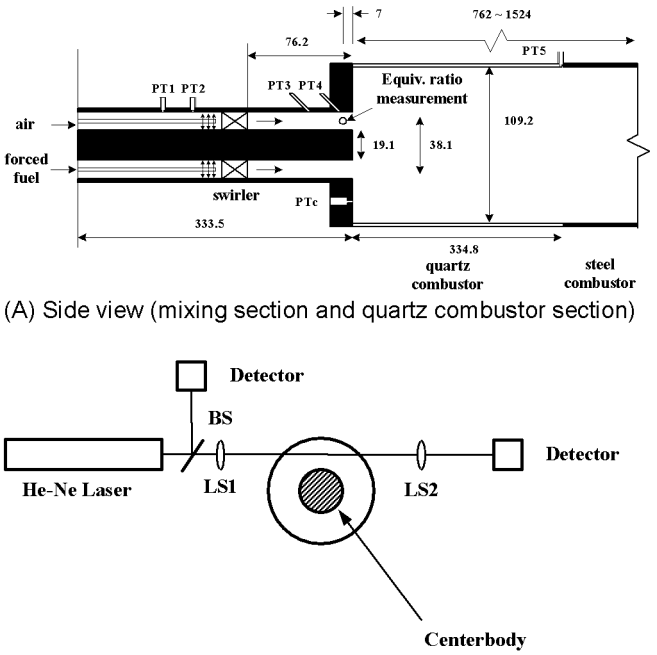

(A) Side view (mixing section and quartz combustor section)

(B) Schematic drawing of experimental setup for equivalence ratio measurements.

Figure 2. Schematic of a swirl-stabilized, lean-premixed, gas turbine combustor. Dimensions in millimeters.

ally examined. Fuel modulation is used to induce mixture ratio perturbations of significant amplitudes at the combustor inlet, while the amplitude of the velocity perturbations is kept negligible, due to the high ratio of air to fuel flow rates. Therefore, the effect of velocity disturbances and large scale vortex structures on the flame's heat release response is not considered here. The present article begins with the details of the operating conditions. Results of the measurements are described and interpreted in the Results and Discussion section. And lastly, linear and nonlinear responses of the flame are interpreted based on phase-resolved CH* chemiluminescence images and nonlinear flame transfer function measurements.

EXPERIMENTAL METHODS

Model Lean-Premixed Gas Turbine Combustor

A schematic drawing of the experimental setup is shown in Figure 2. The combustor consists of an air inlet section, a fuel siren, a mixing section, an optically-accessible quartz combustor section, a steel combustor section, and an exhaust section. The air can be heated to a maximum temperature of 400°C by a 30 kW electric heater. A small-size siren-type modulation device driven by a DC motor was used to modulate the fuel flow rate. The device consists of a rotor (# of holes = 12, d_{hole} = 1.5 mm) and a stator (# of holes = 1, d_{hole} = 1.5 mm). A needle valve was used to adjust the bypass fuel flow

rate, thereby changing the amplitude of modulation ($\Phi'/\overline{\Phi}$) at a given frequency. Modulated fuel is injected into the mixing section and mixed with steady-flow, high-temperature air, leading to equivalence ratio oscillations in the mixing section. The fuel injector has a ring-shaped configuration with 24 holes with d_{hole} = 0.5 mm on its circumference with equal spacing, and it is located 152 mm upstream of the combustor dump plane. The fuel flow rate is not choked so that modulation amplitudes are high enough for the nonlinear flame response study. The mixing section is 0.333 m long and has an annular cross-section with an outer diameter of 38.1 mm. The centerbody with a diameter of 19.2 mm is used for flame stabilization. It is centered in the mixing tube and is positioned such that its downstream end is flush with the combustor dump plane. A 30° flat-vane axial swirler with 6 vanes is mounted in the mixing section 76.2 mm upstream of the combustor dump plane. The swirl vanes provide swirling flow fields to enhance mixing of fuel and air and to stabilize the flame. At the entrance to the mixing section the flow is choked to decouple acoustic fields between the system and the upstream plenum.

The combustor consists of a stainless steel dump plane, to which an optically accessible fused-silica combustor (ID = 109.2 mm and L = 334.8 mm) is attached. The downstream end of the quartz combustor is connected to a stainless steel variable-length combustor section. The length of the combustor can be continuously varied between 762 mm and 1524 mm by moving a water-cooled plug along the length of the steel combustor section. For forced response measurements, the combustor length was maintained at its minimum to minimize the influence of system acoustics on upstream forcing.

Instrumentation and Test Conditions

Several measurement techniques were used to characterize the convective-acoustic perturbations in the mixing plenum and the flame's response to upstream excitation. High frequency-response, water-cooled, piezoelectric pressure transducers (PCB 112A04) were used to measure pressure perturbations in the mixing and the combustor sections. The pressure signals were amplified by charge amplifiers, digitized by an analog-to-digital converter, and stored in microcomputer memory for processing at a sampling rate of 8192 Hz. Pressure signals measured from the two pressure transducers located 12.7 mm (PT4) and 50.8 mm (PT3) upstream of the combustor dump plane were used to estimate the inlet velocity fluctuations using the two-microphone method [21-22]. The measured velocity was used to ensure that fuel modulation does not produce perturbations of acoustic velocity at the inlet of the combustion chamber. To calibrate the two-microphone method, direct measurements of velocity fluctuations were performed under cold flow conditions with a hot wire anemometer (TSI 1210-20). A photomultiplier tube (PMT, Hamamatsu model H7732-10) coupled with a bandpass interference filter (432 ± 5 nm) was used to measure the global CH* chemiluminescence emission intensity from the whole flame. An ICCD camera (Princeton Instruments model 576G) with a CH* bandpass filter centered at 430 nm (10 nm FWHM) was used to record phase-averaged flame images. The ICCD camera was synchronized with the combustor pressure signal and phase-synchronized images were taken over a cycle of oscillation with a phase interval of 30°. The phase angle φ = 0° corresponds to the positive-to-negative zero transition, and φ = 270° to the maximum combustor pressure. Because CH* chemiluminescence images are line-of-sight integrated images, a three-point Abel deconvolution scheme was used to extract two-dimensional information from the line-of-sight images.

Temporal variations of equivalence ratio at the combustor inlet were measured using the infrared (IR) laser absorption technique, which relates the radiation intensities of the laser beam before and after passing through a medium of interest [23]. Figure 2 (B) shows a schematic of the experimental setup for equivalence ratio measurements using the IR absorption technique. A He-Ne laser provides a coherent source of radiation with wavelength of 3.39 μm. The intensity of light is detected by thermoelectrically cooled indium-arsenide (InAs) detectors. The measurement point is located 7 mm upstream of the combustor dump plane. Two different lenses (focal length: LS1 = 533 mm, LS2 = 51 mm) were used to focus the laser beam onto the sensing area (ϕ = 2 mm) of the indium-arsenide detectors.

Experimental data were recorded with a National Instruments data acquisition system controlled by Labview software. A total of 16,384 data points at a sampling rate of 8192 Hz were taken during each test, resulting in a frequency resolution of 0.5 Hz and a time resolution of 0.122 msec. Spectral analysis of the signals was performed using the fast Fourier transform (FFT) technique.

All tests were performed at a mean pressure of 1 atm and at mean equivalence ratios from 0.55 to 0.65. The mean velocity in the mixing section was 60 m/s and the inlet temperature was kept constant at 200 °C, giving a Reynolds number of approximately 33,000. Natural gas and air were used as fuel and oxidizer, respectively. The fuel flow rate modulation frequencies were varied from 100 to 400 Hz (Δf = 25 Hz). The frequency range of 100 to 400 Hz includes two distinct frequencies at which self-excited instabilities were observed in the combustor [24]. Forcing amplitudes were varied from a minimum near zero to a maximum, which in most cases, was limited by lean blowoff.

RESULTS AND DISCUSSION

Flame Transfer Function Measurements

The heat release response of natural gas-air premixed flames to mixture ratio oscillations was determined experimentally for various levels of equivalence ratio oscillation. This section describes the amplitude and frequency dependence of the flame's response to equivalence ratio oscill-

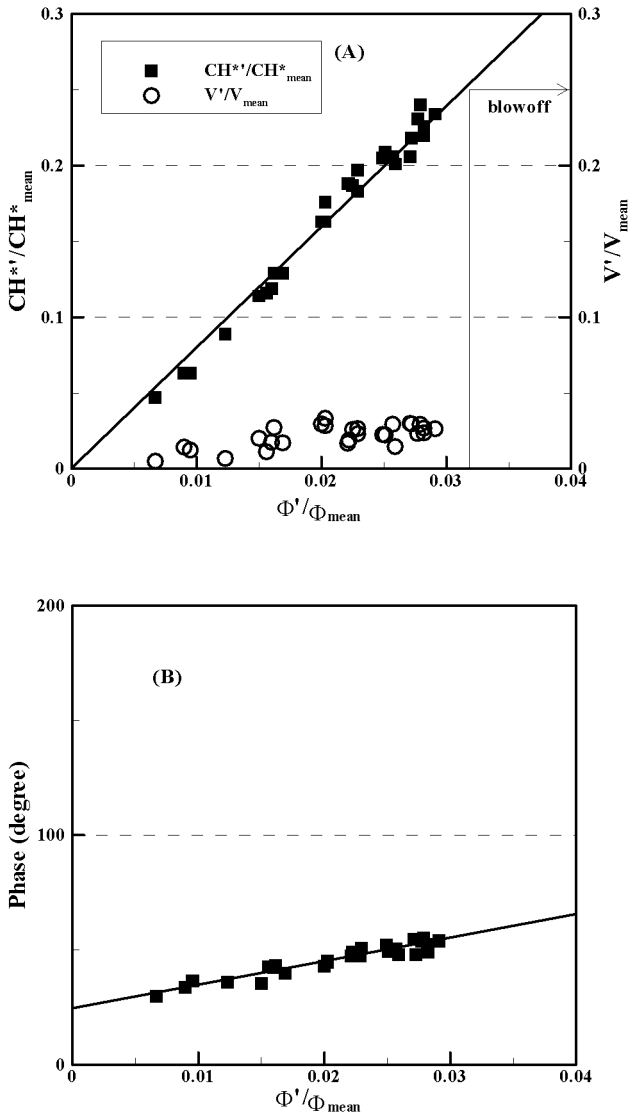

Figure 3. (A) Normalized CH* chemiluminescence intensity and (B) phase of the flame transfer function at a modulation frequency of 100 Hz. Inlet conditions: T_{in} = 200 °C, V_{mean} = 60 m/s, and Φ_{mean} = 0.60.

ations. The dependence of the linear/nonlinear response of the flame upon mean equivalence ratio will be discussed.

To generate equivalence ratio perturbations, mass fractions of either air or fuel must be modulated. If the mass flow rate of fuel is modulated and the mass flow rate of air is kept constant ($\dot{m}_a' = 0$), the amplitude of equivalence ratio oscillations is directly related to that of the fuel mass flow rate:

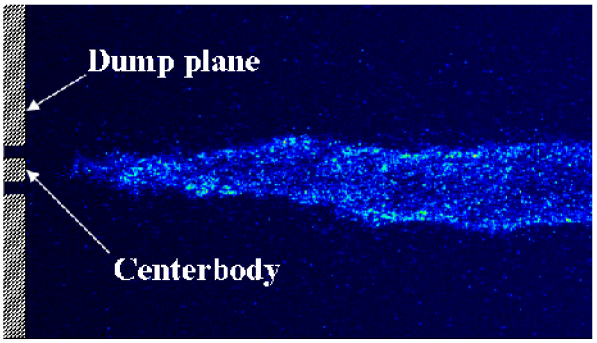

Figure 4. Instantaneous CH* chemiluminescence image at a modulation frequency of 100 Hz and $\Phi'/\bar{\Phi}$ = 4.3%. Inlet conditions: T_{in} = 200 °C, V_{mean} = 60 m/s, and Φ_{mean} = 0.55.

$$\left(\frac{\Phi'}{\bar{\Phi}}\right) = \frac{\frac{\dot{m}_f'}{\bar{m}_f} - \frac{\dot{m}_a'}{\bar{m}_a}}{1 + \frac{\dot{m}_a'}{\bar{m}_a}} = \frac{\dot{m}_f'}{\bar{m}_f} \qquad (1)$$

The term on the left indicates the normalized equivalence ratio oscillations, the flame transfer function input, which was measured using the infrared (IR) absorption technique, as described in the previous section. It was assumed that the radial spatial distribution of the fuel and air mixture is uniform, because of the fuel injector design. This is consistent with the use of the infrared absorption technique to measure the equivalence ratio oscillation, since it is a line-of-sight measurement. The output of the flame transfer function, the heat release rate oscillation, was determined by measuring the intensity of the flame chemiluminescence emission. Chemiluminescence intensity is directly related to the heat release rate of the flame, since fuel flow rates are modulated to generate mixture rate disturbances. To quantitatively describe the response of the flame to mixture ratio oscillations, the flame transfer function is defined as the ratio of the normalized heat release and equivalence ratio fluctuations:

$$H(f,A) = \frac{Q'(f)/\bar{Q}}{\Phi'(f)/\bar{\Phi}} \qquad (2)$$

where $\bar{Q}$ is the time-averaged heat release rate, $\bar{\Phi}$ is the mean equivalence ratio in the mixing section, $Q'(f)$ and $\Phi'(f)$ are the amplitudes of the heat release and equivalence ratio oscillations at the oscillation frequency, f, and A is the magnitude of normalized equivalence ratio oscillation ($\Phi'(f)/\bar{\Phi}$).

A typical example of the flame's heat release response to equivalence ratio modulation is shown in Figure 3, which presents the normalized CH* chemiluminescence fluctuation intensity ($CH^{*\prime}/CH^*_{mean}$) and the phase of the flame transfer

function versus the normalized magnitude of the equivalence ratio oscillation at a modulation frequency of 100 Hz. These measurements were made at an inlet temperature of 200 °C, a mean nozzle velocity of 60 m/s, and a mean equivalence ratio of 0.60. It can be observed that the amplitude of the inlet velocity fluctuations is less than 3% of the mean velocity, even at the maximum amplitude of fuel modulation. This indicates that the influence of inlet velocity fluctuations on heat release oscillations is negligible, and therefore the response of the flame is essentially determined by mixture ratio modulations.

Figure 3 (A) shows that the heat release response increases almost linearly with an increase in the amplitude of the equivalence ratio oscillation, up to Φ'/Φ_{mean} = 3%. This represents the linear flame response at relatively low forcing frequency: the gain is nearly constant with respect to modulation amplitude. It is noteworthy that the maximum driving amplitude point is not determined by a limitation of the modulating device, but by flame blowoff. When the amplitude of mixture ratio perturbations is greater than 3%, the flame becomes detached from the centerbody and lean blowoff occurs. The fact that combustion cannot be sustained at large amplitude equivalence ratio fluctuations suggests that the dynamic flammability limit, defined as the minimum equivalence ratio above which the unsteady flame can sustain combustion [25], depends on the inlet flow conditions.

An example of the flame's shape near blowoff is shown in Figure 4. It shows an instantaneous CH* chemiluminescence image taken at a modulation frequency of 100 Hz and a normalized equivalence ratio fluctuation of 4.3%. The gate width of the ICCD camera was set at 0.833 msec, which corresponds to $T_{acs}/12$. It can be observed that the flame exhibits a tornado-like vortex core structure. The flame is highly unsteady and it is detached from the centerbody. It is believed that incomplete combustion near the lean blowoff point is a major source of pollutant emissions. Therefore, the dependence of the dynamic flammability limits and transient behavior near LBO upon inlet disturbance conditions needs to be elucidated. This work is left for future studies.

Figure 3 (B) shows that the phase difference between the heat release rate and equivalence ratio oscillation gradually increases with an increase in the amplitude of the normalized equivalence ratio fluctuation. This is in contrast to previous results of the flame response to inlet velocity fluctuations, where it was found that the phase of the flame transfer function was independent of the amplitude of the normalized velocity fluctuation for all forcing frequencies [24]. The experimental results shown in Figure 3 (B) indicate that the time required for the flame to respond to Φ' oscillations gradually increases with perturbation amplitude (Φ'/Φ_{mean}). This suggests that temporal evolution of flame surface may be significantly affected by the amplitude of the equivalence ratio disturbance. That issue will be analyzed in detail in this section using phase-resolved CH* chemiluminescence images. Note that some scatter is observed in the data shown in Figure 3. This may be due to uncertainties related to the IR absorption technique, such as the inherent random noise of a He-Ne laser beam. The trend of the variation is nevertheless well captured.

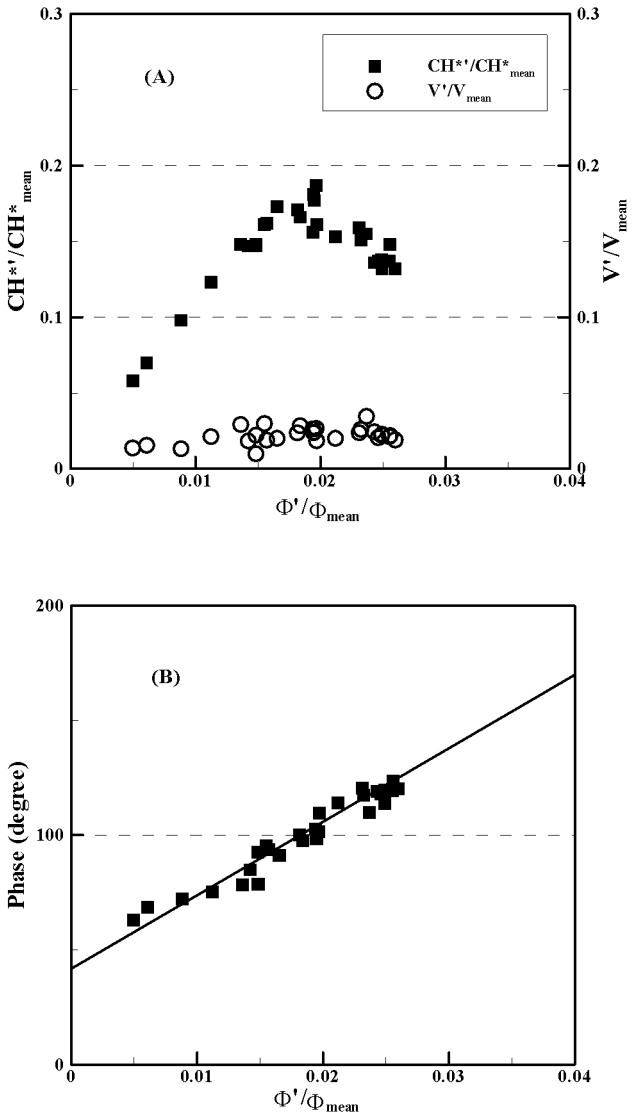

Figure 5. (A) Normalized CH* chemiluminescence intensity and (B) phase of the flame transfer function at a modulation frequency of 150 Hz. Inlet conditions: T_{in} = 200 °C, V_{mean} = 60 m/s, and Φ_{mean} = 0.60.

The heat release response at a modulation frequency of 150 Hz is plotted against perturbation amplitude in Figure 5. The plot shows that the response increases linearly up to Φ'/Φ_{mean} = 2%, and then starts to decrease with increasing modulation amplitude. This is a typical example of the nonlinear response of a flame subjected to Φ' perturbations:

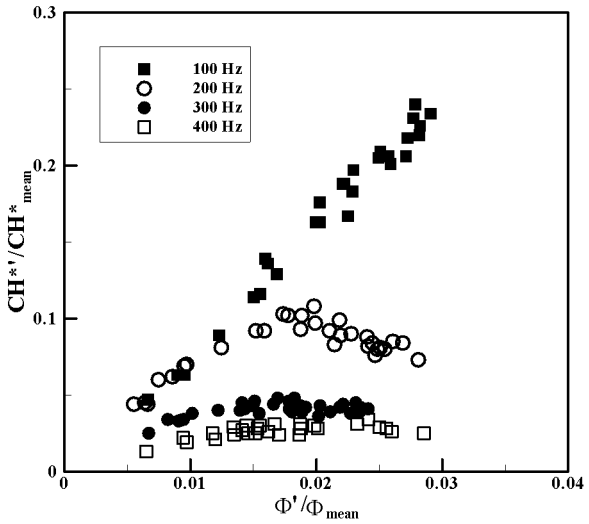

Figure 6. Dependence of the normalized CH* chemiluminescence intensity fluctuation on the modulation frequency. Inlet conditions: T_{in} = 200 °C, V_{mean} = 60 m/s, and Φ_{mean} = 0.60.

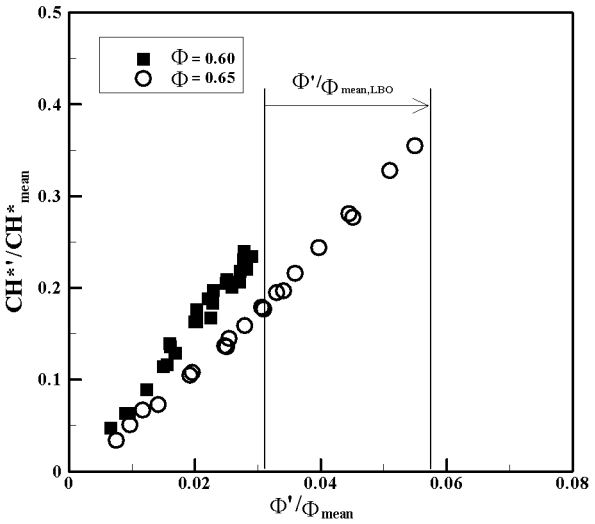

Figure 7. Dependence of the response of a flame upon mean equivalence ratio at a modulation frequency of 100 Hz. Inlet conditions: T_{in} = 200 °C, V_{mean} = 60 m/s, and Φ_{mean} = 0.60, 0.65.

after a certain point the gain starts to level off or decrease with increasing normalized equivalence ratio fluctuation, Φ'/Φ_{mean}. The mechanisms responsible for the observed nonlinear behavior will be discussed when the phase-locked flame images are presented. It should be noted that as in the prior case (Fig. 3), the phase gradually increases with increasing amplitude, indicating that the effective flame length increases with modulation amplitude. Note that the normalized velocity fluctuation is less than 3%, indicating that the nonlinear response of the flame is caused by equivalence ratio fluctuations.

It can be seen from Figures 3 (100 Hz) and 5 (150 Hz) that the nonlinearity occurs at lower Φ'/Φ_{mean} as the modulation frequency increases. The flame response is linear up to Φ'/Φ_{mean} = 3% at a frequency of 100 Hz, while the nonlinear response is observed at Φ'/Φ_{mean} = 2% at a frequency of 150 Hz. Figure 6 shows the dependence of the normalized CH* chemiluminescence intensity on the modulation frequency between 100 and 400 Hz. It is evident from Figure 6 that the normalized CH* chemiluminescence intensity fluctuation decreases with increasing excitation frequency, at a fixed perturbation amplitude, and the flame's response at modulation frequencies of 300 and 400 Hz is nonlinear over the range of equivalence ratio fluctuation tested. Although the controlling physics of the nonlinear response to equivalence ratio fluctuations is totally different than the controlling physics of the nonlinear response to velocity fluctuations, the fact that the perturbation amplitude at which the nonlinear response occurs decreases with increasing frequency is observed in both cases. The dependence of the inception of the nonlinear response on modulation frequency shows the same trend [17, 26].

In summary, the above results indicate that the effect of modulation frequency on the flame response to both velocity and equivalence ratio fluctuations is qualitatively similar, although the flame response to equivalence ratio and to velocity fluctuations are quantitatively very different.

The normalized CH* chemiluminescence intensity fluctuation is an order of magnitude greater for equivalence ratio fluctuations than for velocity oscillations. Furthermore, the nonlinear response occurs at smaller normalized equivalence ratio fluctuations (e.g., Φ'/Φ_{mean} ~ 2% for 200Hz modulation) than normalized velocity fluctuations (e.g., V'/V_{mean} ~20% for 200 Hz modulation). When the flame is perturbed by inlet velocity oscillations, high amplitude perturbations are required for shear layer rollup, leading to shedding of a coherent vortex-ring structure. Flame area modulation induced by flame-vortex interaction thus leads to the nonlinear response of heat release oscillations. On the other hand, equivalence ratio modulations directly affect the heat release rate, by means of variations in burning velocity and the heat of reaction of the incoming reactants. Perturbations of flame surface area are also indirectly induced by the burning velocity fluctuations [12].

The dependence of the flame's response upon mean equivalence ratio at a modulation frequency of 100 Hz is illustrated in Figure 7. As the mean equivalence ratio increases from 0.60 to 0.65, the magnitude of the heat release response decreases for a constant amplitude of perturbation, and the response remains in the linear region for both cases. This is at-

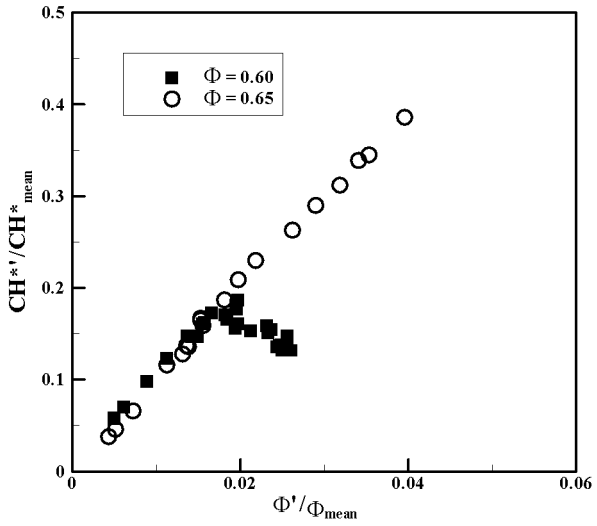

Figure 8. Dependence of the response of a flame upon mean equivalence ratio at a modulation frequency of 150 Hz. Inlet conditions: T_{in} = 200 °C, V_{mean} = 60 m/s, and Φ_{mean} = 0.60, 0.65.

tributed to the enhanced flame stiffness, as mean equivalence ratio increases. When the mean equivalence ratio is near the static lean blowoff limit, on the other hand, the flame is more easily destabilized when subjected to upstream disturbances.

It is also noted that the dynamic flammability limit is extended from Φ'/Φ_{mean} ~ 3% to 6% with increasing mean equivalence ratio. This is consistent with results of Sankaran and Im [25]. They computationally studied the response of an unsteady premixed methane/air flame subjected to time-varying composition fluctuations and concluded that the flammability limit is extended to lower equivalence ratios as the mean equivalence ratio increases or the characteristic frequency of oscillation increases.

Figure 8 shows the effects of mean equivalence ratio on the response of the flame at a modulation frequency of 150 Hz. It is evident that the flame at a mean equivalence ratio of 0.60 exhibits nonlinear behavior, while the flame at Φ_{mean} = 0.65 shows linear response characteristics. This is associated with the improved stability characteristic of the flame as mean equivalence ratio increases. Note that the dynamic flammability limits are also extended by approximately 60%, as mean equivalence ratio increases from 0.60 to 0.65.

The results shown in Figures 7 and 8 suggest that the linear/nonlinear dynamics of a flame submitted to equivalence ratio oscillations are strongly dependent on the mean equivalence ratio. As the mean equivalence ratio decreases, e.g., when Φ_{mean} is near the static LBO limit, the nonlinear response of a flame to equivalence ratio perturbations is more prominent. This could be due to the fact that near the lean blo-

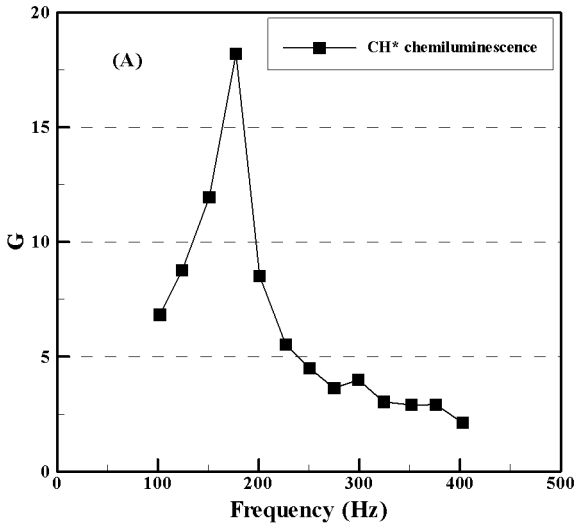

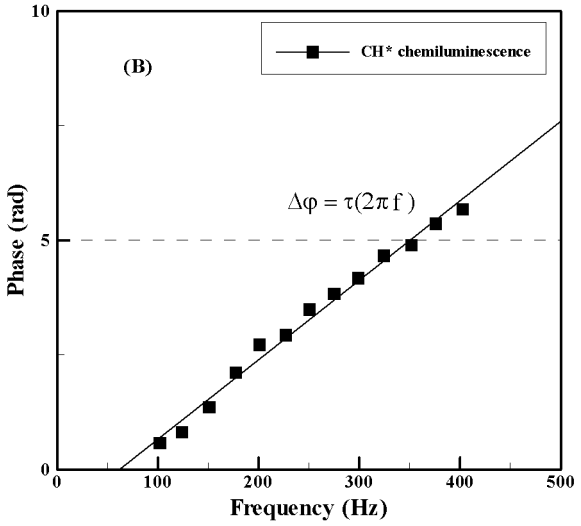

Figure 9. (A) Gain and (B) phase of the flame transfer function in frequency domain. Inlet conditions: T_{in} = 200 °C, V_{mean} = 60 m/s, Φ_{mean} = 0.60, and Φ'/Φ_{mean} = 1%.

woff limit the burning rate and heat of reaction are nonlinearly related to equivalence ratio. A similar observation was made by Shreekrishna and Lieuwen [27]. They showed that the key mechanism leading to heat release saturation is the intrinsically nonlinear dependence of flame speed and mixture heat of reaction on fuel/air ratio.

The gain and phase of the flame transfer function can be expressed in the frequency domain at the same magnitude of equivalence ratio perturbations Φ'/Φ_{mean} = 1%. This amplitude limits the flame response to the linear region. Figure 9 plots

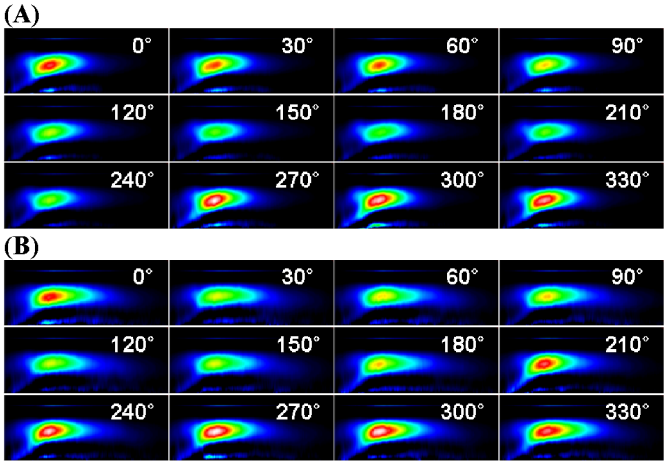

Figure 10. Phase-resolved CH* chemiluminescence imaging during a period of oscillation at a modulation frequency of 200 Hz and amplitudes of (A) $\Phi'/\overline{\Phi}$ = 2.2% and (B) $\Phi'/\overline{\Phi}$ = 3.2%. Inlet conditions: T_{in} = 200 °C, V_{mean} = 60 m/s, and Φ_{mean} = 0.60.

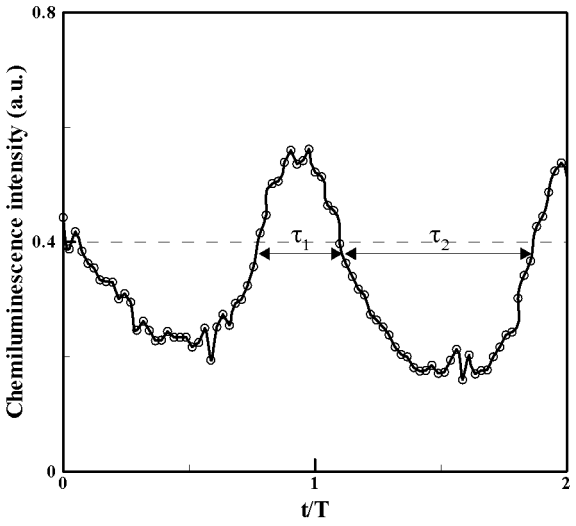

Figure 11. Time signal of CH* chemiluminescence intensity at a modulation frequency of 200 Hz and amplitude of $\Phi'/\overline{\Phi}$ =2.2%. Inlet conditions: T_{in} = 200 °C, V_{mean} = 60 m/s, and Φ_{mean} = 0.60.

the flame transfer function against modulation frequency for a mean equivalence ratio of 0.60 and a mean inlet velocity of 60 m/s. The flame transfer function exhibits a low-pass filter behavior, as when the flame area is influenced by acoustic velocity perturbations. It can be seen from Figure 9 (A) that a strong overshoot at a modulation frequency of 175 Hz is observed and the gain asymptotically decreases to zero with increasing modulation frequency. The physical significance of this result is that the flame selectively amplifies equivalence ratio perturbations within certain frequency ranges. The frequency where the response of the flame is most amplified is consistent with one of self-excited instability frequencies observed in the test rig [24]. A small peak at a frequency of 300 Hz is also observed in Fig 9(A). A similar phenomenon has also been observed in numerical investigations [12].

Figure 9 (B) shows the corresponding phase of the flame transfer function, which provides the convection times needed for the flame to respond to upstream equivalence ratio perturbation. The overall time delay consists of a characteristic time delay for the convective transport of the equivalence ratio perturbation from the combustor inlet to the main reaction zone, a time delay for the heating of the reactant mixtures to ignition temperature, and a characteristic kinetic time delay for the chemical reaction. It can be seen from Figure 9 (B) that the phase difference between Φ' and CH*′ evolves quasi-linearly with frequency, $\Delta\varphi = \tau(2\pi f)$. This phase dependence indicates a roughly constant time delay (τ) between the equivalence ratio perturbation (Φ') and the heat release perturbation (CH*′), which implies that their relationship is purely convective in nature. The global flame transfer functions subjected to equivalence ratio oscillations show many similarities to the flame's response to acoustic (velocity) perturbations, in terms of both the gain and the phase (time delay).

Nonlinear Flame Dynamics

This section describes the nonlinear features of a flame subjected to equivalence ratio modulation. Phase-averaged CH* chemiluminescence flame images were measured using an ICCD camera at phase intervals of 30°. Figure 10 shows phase-averaged CH* chemiluminescence images during a cycle of oscillation at a modulation frequency of 200 Hz with a normalized equivalence ratio fluctuation of 2.2% (A) and 3.2% (B). The intensity of the CH* chemiluminescence emission is highest at φ = 270° for both cases. No shear layer rollup is seen, due to the low amplitude of the velocity perturbation at the combustor inlet; the heat release oscillations are caused by equivalence ratio fluctuations. Figure 11 plots a time series of the global CH* chemiluminescence, measured by the photomultiplier tube. This corresponds to the flame dynamics shown in Figure 10 (A). It clearly shows that the heat release signal varies significantly. The waveform features nonlinear behavior, since a sharp peak of heat release is produced in each cycle ($\tau_2 \gg \tau_1$). Birbaud et al. [19] observed similar phenomena. They found that the flame behaves like a relaxation oscillator, with slow growth followed by a sharp drop.

It is noteworthy (see Figure 10 (A)) that the overall flame length is almost constant over a cycle of oscillation at a given perturbation amplitude. This suggests that the influence of the variation in heat of reaction upon the heat release rate oscillation is more significant than that of flame speed. If the

flame speed varies substantially during a period of oscillation, the flame length change will be prominent; $L_{flame} \propto S_T$ (S_T = turbulent flame speed). This behavior is similar to the Large Eddy Simulation (LES) results of Sengissen et al. [20]. They found that the flame does not move significantly when the equivalence ratio modulation impinges on the swirl-stabilized flame.

Figure 10 (B) shows phase-resolved CH* chemiluminescence images over a period of oscillation (200 Hz) for a normalized equivalence ratio fluctuation of 3.2%. This forcing condition is very close to the dynamic blowoff limit. The flame length, at a given phase, is longer in this case than it is for a normalized equivalence ratio fluctuation of 2.2% (Fig. 10(A)). The fact that increasing the normalized equivalence ratio fluctuation increases the flame length, as shown in Fig. 10, indicates that the time required for the equivalence ratio perturbation to convect from the dump plane to the flame should increase with increasing normalized equivalence ratio fluctuation. This is consistent with the effect of the normalized equivalence ratio fluctuation on the transfer function phase shown in Fig. 5(B). The nonlinear dynamics of the flame results in enhanced unsteadiness near blowoff. However, unsteady local extinction events, which are known to be the first stage of near-blowoff dynamics of bluff-body stabilized flames, are not observed here [28]. This indicates that the instantaneous stretch rate does not exceed the local extinction stretch rate.

CONCLUSIONS

Even though it is well understood that temporal oscillations in the equivalence ratio play an important role in inducing self-sustained pressure oscillations in lean-premixed gas turbines, this key issue has not been well explored experimentally. Results are presented in this paper from an experimental study of the response of swirl-stabilized flames to equivalence ratio oscillations. Equivalence ratio perturbations were achieved by modulating the fuel flow rate, giving nearly sinusoidal equivalence ratio oscillations at the combustor inlet. It was found that the response of the flame can be divided into linear and nonlinear regimes, depending on the magnitude of the equivalence ratio oscillations. For large perturbation amplitudes, the heat release response shows nonlinear behavior with abrupt changes in the waveform. The nonlinearity is related to the nonlinear dependence of the heat of reaction and burning velocity on equivalence ratio. The nonlinear response becomes more pronounced as modulation frequencies increase and the mean equivalence ratio decreases. It was also found that the flame acts as an amplifier of equivalence ratio perturbations at modulation frequencies of approximately 175 Hz and that the measured phase between the CH* chemiluminescence intensity and the inlet equivalence ratio oscillations increases linearly with excitation frequency. This suggests that the overall characteristics of the flame's response to equivalence ratio oscillations are very similar to the flame's response to velocity fluctuations, although the mechanism responsible for the nonlinear behavior is different. The data presented in the present paper provides insight into the physics controlling the response of the flame to equivalence ratio modulation and can be used to validate analytic flame response models.

ACKNOWLEDGMENT

Funding for this research was provided by the Department of Energy University Coal Research Program through Contract # DE-FG26-07NT43069 and the National Science Foundation through Award #0625970.

REFERENCES

[1] Lieuwen, T. and Yang, V., 2005, "Combustion Instabilities in Gas Turbine Engines," Progress in Astronautics and Aeronautics, vol. 210, AIAA, Washington, DC.

[2] Candel, S., 2002, "Combustion dynamics and control: progress and challenges," Proc. Combust. Instit., **29**, pp. 1-28.

[3] Ducruix, D., Schuller, T., Durox, D., and Candel. S., 2003, "Combustion dynamics and instabilities: elementary coupling and driving mechanisms," J. Propul. Power, **19,** pp. 722-734.

[4] Fleifil, M., Annaswamy, A.M., Ghoneim, Z.A., and Ghoniem, A.F., 1996, "Response of a laminar premixed flame to flow oscillations: a kinematic model and thermoacoustic instability results," Combust. Flame, **106**, pp. 487-510.

[5] Venkataraman, K.K., Preston, L.H., Simons, D.W., Lee, B.J., Lee, J.G., and Santavicca, D.A., 1999, "Mechanism of combustion instability in a lean premixed dump combustor," J. Propul. Power, **15**, (6), pp. 909-918.

[6] Yu, K., Trouve, A., and Daily, J., 1991, "Low-frequency pressure oscillations in a model ramjet combustor," J. Fluid Mech., **232**, pp. 47-72.

[7] Schadow, K.C. and Gutmark, E., 1992, "Combustion instability related to vortex shedding in dump combustors and their passive control," Prog. Energy Combust. Sci., **18**, pp. 117-132.

[8] Poinsot, T.J., Trouve, A.C., Veynante, D.P., Candel, S.M., and Esposito, E.J., 1987, "Vortex-driven acoustically coupled combustion instabilities," J. Fluid Mech., **177**, pp. 265-292.

[9] Schuller, T., Durox, D., and Candel, S., 2002, "Dynamics of and noise radiated by a perturbed impinging premixed jet flame," Combust. Flame, **128**, pp. 88-110.

[10] Lee, J.G., Kim, K., and Santavicca, D., 2000, "Measurement of equivalence ratio fluctuation and its effect on heat release during unstable combustion," Proc. Combust. Inst., **28**, pp. 415-421.

[11] Lieuwen, T. and Zinn, B., 1998, "The role of equivalence ratio oscillations in driving combustion instabilities in low NOx gas turbines," Proc. Combust. Inst., **27**, pp. 1809-

1816.
[12] Cho, J. and Lieuwen, T., 2005, "Laminar premixed flame response to equivalence ratio oscillations," Combust. Flame, **140**, pp. 116-129.
[13] Sattelmayer, T., 2003, "Influence of the combustor aerodynamics on combustion instabilities from equivalence ratio fluctuations," ASME J. Eng. Gas Turb. Power, **123**, pp. 11-19.
[14] Balachandran, R., Ayoola, B.O., Kaminski, C.F., Dowling, A.P., and Mastorakos, E., 2005, "Experimental investigation of the nonlinear response of turbulent premixed flames to imposed inlet velocity oscillations," Combust. Flame, **143**, pp. 37-55.
[15] Bellows, B.D., Neumeier, Y., and Lieuwen, T., 2006, "Forced response of a swirling, premixed flame to flow disturbances," J. Propul. Power, **22**, pp. 1075-1084.
[16] Kang, D.M., Culick, F.E.C., and Ratner, A., 2007, "Combustion dynamics of a low-swirl combustor," Combust. Flame, **151**, pp. 412-425.
[17] Kulsheimer, C. and Buchner, H., 2002, "Combustion dynamics of turbulent swirling flames," Combust. Flame, **131**, pp. 70-84.
[18] Armitage, C.A., Balachandran, R., Mastorakos, E., and Cant, R.S., 2006, "Investigation of the nonlinear response of turbulent premixed flames to imposed inlet velocity oscillations," Combust. Flame, **146**, pp. 419-436.
[19] Birbaud, A., Ducruix, S., Durox, D., and Candel, S., 2008, "The nonlinear response of inverted "V" flames to equivalence ratio nonuniformities," Combust. Flame, **154**, pp. 356-367.
[20] Sengissen, A.X., Van Kampen, J.F., Huls, R.A., Stoffels, G.G.M., Kok, J.B.W., and Poinsot, T.J., 2007, "LES and experimental studies of cold and reacting flow in a swirled partially premixed burner with and without fuel modulation," Combust. Flame, **150**, pp. 40-53.
[21] Waser, M.P. and Crocker, M.J., 1984, "Introduction to the two-microphone cross-spectral method of determining sound intensity," Noise Control Eng. J., **22**, pp. 76-85.
[22] Abom, M. and Boden, H., 1988, "Error analysis of two-microphone measurements in ducts with flow," J. Acoust. Soc. Am., **83**, pp. 2429-2438.
[23] Lee, J.G. and Santavicca, D.A., 2003, "Experimental diagnostics for the study of combustion instabilities in lean premixed combustors," J. Propul. Power, **19**, pp. 735-750.
[24] Kim, K.T., Lee, H.J., Lee, J.G., Quay, B., and Santavicca, D., 2009, "Flame transfer function measurement and instability frequency prediction using a thermoacoustic model," ASME paper GT2009-60026.
[25] Sankaran, R. and Im, H.G., 2002, "Dynamic flammability limits of methane/air premixed flames with mixture composition fluctuations," Proc. Combust. Instit., **29**, pp. 77-84.
[26] Kim, D., Lee, J.G., Quay, B.D., and Santavicca, D.A., 2008, "Effect of flame structure on the flame transfer function in a premixed gas turbine combustor," ASME paper GT2008-51014.
[27] Shreekrishna, S.H. and Lieuwen, T., 2007, "Premixed flame response to equivalence ratio perturbations," 43rd AIAA/ASME/ASEE Joint Propulsion Conference, AIAA paper #2007-5656.
[28] Nair, S. and Lieuwen, T., 2007, "Near-blowoff dynamics of a bluff-body stabilized flame," J. Propul. Power, **23**, pp. 421-427.